11

12

13

14

15

16

17

18

19

20

21

22

23

24

26

27

28

29

30

31

# Bioverse: Potentially Observable Exoplanet Biosignature Patterns Under the UV Threshold Hypothesis for the Origin of Life

Martin Schlecker D, Dániel Apai D, 1, 2 Antonin Affholder D, 3 Sukrit Ranjan D, 2, 4 Régis Ferrière D, 3, 5, 6
Kevin K. Hardegree-Ullman D, 1 Tim Lichtenberg D, 7 and Stéphane Mazevet D8

1 Steward Observatory, The University of Arizona, Tucson, AZ 85721, USA; schlecker @arizona.edu

2 Lunar and Planetary Laboratory, The University of Arizona, Tucson, AZ 85721, USA

3 Department of Ecology and Evolutionary Biology, University of Arizona, Tucson AZ, USA

4 Blue Marble Space Institute of Science, Seattle, 98104, USA

5 Institut de Biologie de l'École Normale Supérieure, ENS, PSL, Paris, France

6 International Research Laboratory for Interdisciplinary Global Environmental Studies (iGLOBES), CNRS, ENS, PSL, University of Arizona, Tucson AZ, USA

7 Kapteyn Astronomical Institute, University of Groningen, PO Box 800, 9700 AV Groningen, The Netherlands

8 Observatoire de la Côte d'Azur, Université Côte d'Azur, Nice, France

ABSTRACT

A wide variety of scenarios for the origin of life have been proposed, with many influencing the prevalence and distribution of biosignatures across exoplanet populations. This relationship suggests these scenarios can be tested by predicting biosignature distributions and comparing them with empirical data. Here, we demonstrate this approach by focusing on the cyanosulfidic origins-of-life scenario and investigating the hypothesis that a minimum near-ultraviolet (NUV) flux is necessary for abiogenesis. Using Bayesian modeling and the Bioverse survey simulator, we constrain the probability of obtaining strong evidence for or against this "UV Threshold Hypothesis" with future biosignature surveys. Our results indicate that a correlation between past NUV flux and current biosignature occurrence is testable for sample sizes of  $\gtrsim 50$  planets. The diagnostic power of such tests is critically sensitive to the intrinsic abiogenesis rate and host star properties, particularly maximum past NUV fluxes. Surveys targeting a wide range of fluxes, and planets orbiting M dwarfs enhance the chances of conclusive results, with sample sizes \$\ge 100\$ providing \$\ge 80\% likelihood of strong evidence if abiogenesis rates are high and the required NUV fluxes are moderate. For required fluxes exceeding a few hundred erg/s/cm<sup>2</sup>, both the fraction of inhabited planets and the diagnostic power sharply decrease. Our findings demonstrate the potential of exoplanet surveys to test origins-of-life hypotheses. Beyond specific scenarios, this work underscores the broader value of realistic survey simulations for future observatories (e.g., HWO, LIFE, ELTs, Nautilus) in identifying testable science questions, optimizing mission strategies, and advancing theoretical and experimental studies of abiogenesis.

## 1. INTRODUCTION

A wide variety of scenarios for the origin of life have been proposed (e.g., ??????). While we may still be far from conclusively testing these scenarios, new prospects in the search for conditions favorable to life have opened up by thinking of the origin of life as a planetary phenomenon and identifying global-scale environmental properties that might support pathways to life (?). In particular, specific planetary conditions are needed to create stockpiles of initial compounds for prebiotic chemistry; and planetary processes are required to trigger the prebiotic synthesis. Such planetary conditions can be hypothesized for exoplanets located in the habitable zone (HZ) of their host star, with persistent liquid

water on their surface. For example, if deep-sea or sedimentary hydrothermalism is required for abiogenesis, then the insulation of an ocean from the planetary crust minerals (e.g., due to high-pressure ices) may reduce or eliminate the chances of life emerging (e.g., ?). The alternate scenario of a surface locally subject to wet-dry cycles requires a planetary exposure to mid-range Ultraviolet (UV) irradiation, as a source of energy and an agent of selection in chemical evolution (e.g., ?). This "UV Threshold Hypothesis" states that UV light in a specific wavelength range played a constructive role in getting life started on Earth (????), and it could provide a probabilistic approach to the interpretation of possible future biosignature detections (e.g., ??).

The association of chemical pathways to life and plan-60 etary environmental conditions offers a new opportunity 61 to test alternate scenarios for life emergence based on 62 planetary-level data collected from the upcoming ob-63 servations of populations of exoplanets. Deep-sea hy-64 drothermal scenarios require planetary conditions that 65 may not be met on ocean worlds with large amounts 66 of water, where the water pressure on the ocean floor 67 is high enough to form high-pressure ices (??). In this 68 case, a testable prediction would be that planets with 69 high-pressure ices do not show biosignatures. Likewise, 70 if UV light is required to get life started, then there is 71 a minimum planetary UV flux requirement to have an 72 inhabited world. This requirement is set by competing 73 thermal processes; if the photoreaction does not move 74 forward at a rate faster than the competitor thermal 75 process(es), then the abiogenesis scenario cannot func-76 tion. On the other hand, abundant UV light vastly in 77 excess of this threshold does not increase the probability 78 of abiogenesis, since once the UV photochemistry is no 79 longer limiting, some other thermal process in the reaction network will be the rate-limiting process instead. 81 Therefore, a putative dependence of life on UV light is 82 best described as a step function (e.g., ???).

The goal of this work is to evaluate the potential of future exoplanet surveys to test the hypothesis that a minimum past NUV flux is required for abiogenesis. We focus on one version of the UV Threshold Hypothesis, the so-called cyanosulfidic scenario, which has been refined to the point where the required threshold flux has been measured to be  $F_{\rm NUV,min}=(6.8\pm3.6)\times10^{10}\,{\rm photons\,cm^{-2}\,s^{-1}\,nm^{-1}}$  integrated from 1200–280 nm at the surface (?????).

We follow a semi-analytical Bayesian analysis to es-93 timate probabilities of obtaining strong evidence for or 94 against this hypothesis. Under the UV Threshold Hy-95 pothesis  $(H_1)$ , the probability of an exoplanet having 96 detectable biosignatures is zero if the near-ultraviolet 97 (near-Ultraviolet (NUV)) irradiation is less than the 98 threshold, and it is equal to the (unknown) probability 99 of life emerging and persisting,  $f_{\text{life}}$  if NUV exceeds 100 the threshold for a sufficiently long period of time. Under the null hypothesis  $(H_{\text{null}})$ , that probability simply 102 is  $f_{\text{life}}$ , that is, it does not correlate with the UV flux. Figure ?? shows these hypotheses as derived from the predictions of the cyanosulfidic scenario. Given a sample 106 of planets, where for some of them we have convincing 107 biosignature detections but remain agnostic on  $f_{
m life},$  we ask what evidence for  $H_1$  and  $H_{
m null}$  we can expect to 109 obtain.

A real exoplanet survey will be subject to observational biases and sample selection effects, and will be constrained by the underlying demographics of the planet sample. To assess the information gain of a realistic exoplanet survey, we employed Bioverse (????), a framework that integrates multiple components including statistically realistic simulations of exoplanet populations, a survey simulation module, and a hypothesis testing module to evaluate the statistical power of different observational strategies.

This paper is organized as follows: In Section ??, we introduce both our semi-analytical approach and Bioverse simulations for testing the UV Threshold Hypothesis. Section ?? presents the results of these experiments for a generic survey as well as for a realistic transit survey. In Section ??, we discuss our findings before concluding with a summary in Section ??.

## 2. METHODS

# 2.1. Fraction of inhabited planets with detectable biosignatures

128

129

138

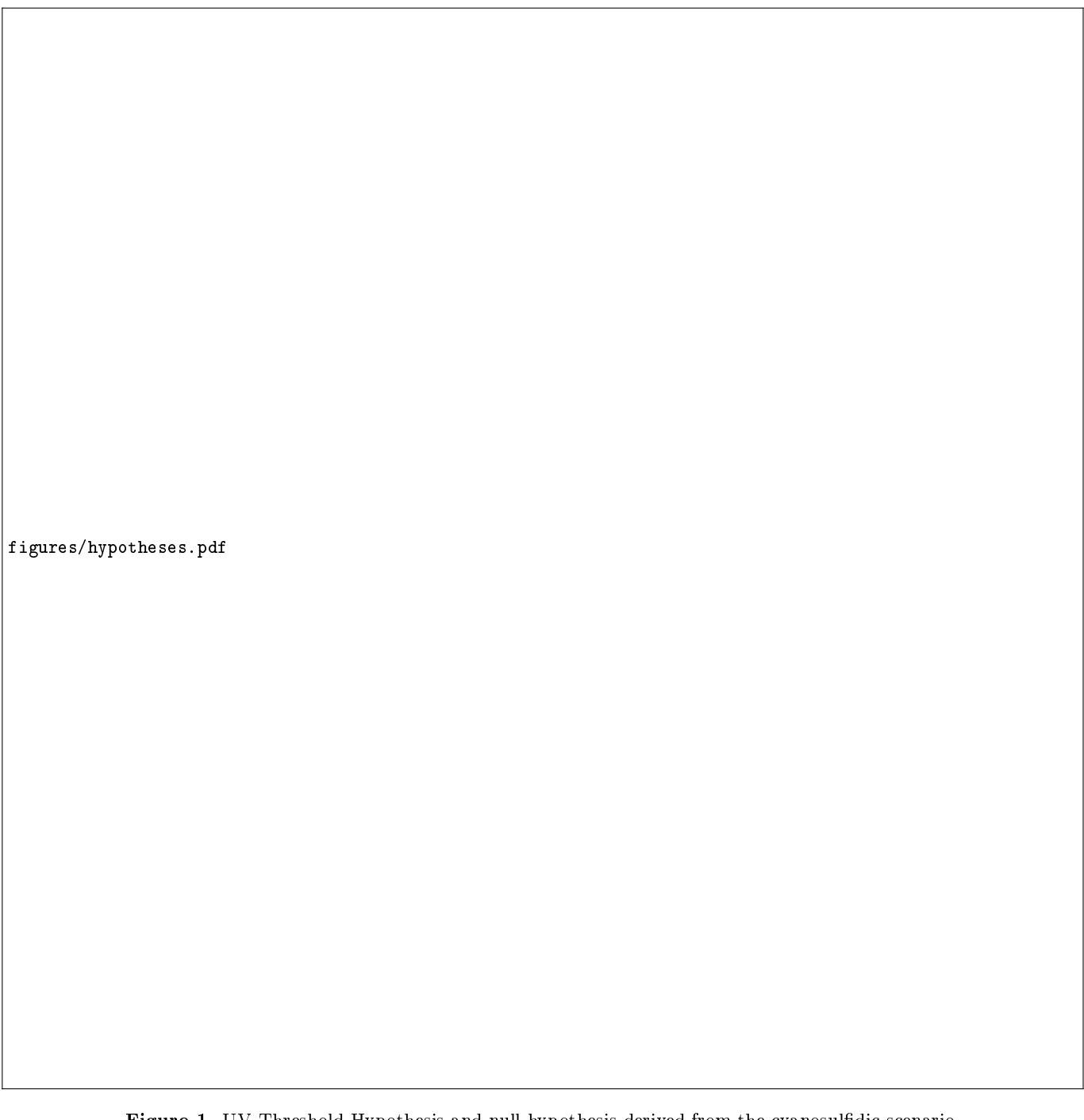
Here, we conduct a theoretical experiment on the UV Threshold Hypothesis by relating the occurrence of life on an exo-earth candidate with a minimum past quisescent stellar UV flux, focusing on the prebiotically interesting NUV range from 200–280 nm (?). Our core hypothesis shall be that life only occurs on planets that at some point in their history have received such radiation at a flux exceeding a threshold  $F_{\rm NUV,min}$ .

## $2.2. \ Semi-analytical\ approach$

We first assessed the expected probabilities of obtaining true negative or true positive evidence for the UV Threshold Hypothesis  $(H_1)$  above, as well as the probability for misleading or inconclusive evidence, under idealized conditions. This serves as a first-order estimate of the information content of a survey, before we take into account the effects of exoplanet demographics, sample selection, and survey strategy.

Presumably, not all habitable worlds are inhabited and not all inhabited worlds develop detectable biosignatures. The fraction of exo-Earth candidates (EEC) that are both inhabited and exhibit detectable biosignatures at the time of observation is unknown and is represented by the term  $f_{\rm life}$ . This encompasses the probability of life both emerging and persisting to produce detectable biosignatures. Let us consider the probability to detect a biosignature P(L), and let our observable be the inferred past NUV flux of the planet  $F_{\rm NUV}$ . Under Hypothesis  $H_1$ , there exists a special unknown value of  $F_{\rm NUV}$ , noted  $F_{\rm NUV,min}$  such that

$$P(L|F_{\text{NUV}}, H_1) = f_{\text{life}} \quad \text{if } F_{\text{NUV}} > F_{\text{NUV,min}}$$
 (1)



 ${\bf Figure~1.~UV~Threshold~Hypothesis~and~null~hypothesis~derived~from~the~cyanosulfidic~scenario.}$ 

 $P(L|F_{\rm NUV},H_1)=0$  otherwise (2) where  $f_{\rm life}$  is the unknown probability of abiogenesis.

161 The corresponding null hypothesis  $H_{\rm null}$  is that there
162 exists no such special value of  $F_{\rm NUV}$  and that

163  $P(L|F_{\rm NUV},H_{\rm null})=f_{\rm life}$ . (3)

 $_{\mbox{\scriptsize 164}}$  In other words,  $H_{\mbox{\scriptsize null}}$  states that P(L) is independent of  $_{\mbox{\scriptsize 165}}$   $F_{\mbox{\scriptsize NUV}}.$ 

Defining a sample of size n as  $X = \{F_{\text{NUV},i}, L_i\}_{i \in [1,n]}$  where  $L_i$  is equal to 1 if life is detected and 0 otherwise,

we can calculate the evidence for hypothesis  $H_i$  being true against  $H_j$  through the Bayes factor

$$BF_{H_i,H_j} = \frac{P(X|H_i)}{P(X|H_j)},\tag{4}$$

with  $P(X|H_i)$  and  $P(X|H_j)$  likelihoods of obtaining the sample X under either hypothesis.

Let  $Y = \sum_{i}^{n} L_{i}$  be the random variable counting the number of positive life detections in a sample of size n.

Its probability mass function under the null hypothesis  $H_{null}$  is that of a binomial distribution:

$$P(Y = k|H_{\text{null}}) = \binom{n}{k} f_{\text{life}}^k (1 - f_{\text{life}})^{n-k}.$$
 (5)

Under  $H_1$ , Y also follows a binomial distribution, howver it is conditioned by  $n_{\lambda} = n(\{F_{\text{NUV},i} \text{ if } F_{\text{NUV},i} > F_{\text{NUV},\min}\}_{i \in [1,n]})$ , the number of values of  $F_{\text{NUV}}$  in the experiment that exceed  $F_{\text{NUV},\min}$ 

$$P(Y = k|H_1) = \binom{n_{\lambda}}{k} f_{\text{life}}^k (1 - f_{\text{life}})^{n_{\lambda} - k}. \tag{6}$$

183 Hence,

$$BF_{H_1,H_{\text{null}}} = \frac{P(Y = k|H_1)}{P(Y = k|H_{\text{null}})} = \frac{\binom{n_{\lambda}}{k}}{\binom{n}{k}} (1 - f_{\text{life}})^{n_{\lambda} - n},$$
(7a)

 $_{185}$  and

$$BF_{H_{\text{null}},H_1} = \frac{P(Y=k|H_{\text{null}})}{P(Y=k|H_1)} = \frac{\binom{n}{k}}{\binom{n_{\lambda}}{k}} (1-f_{\text{life}})^{n-n_{\lambda}}.$$
 (7b)

Given a sample of planets, where for some of them we have convincing biosignature detections but remaining agnostic on  $f_{\rm life}$ : What evidence for  $H_1$  and  $H_{\rm null}$  can we expect to get? The analytical expression for the Bayes factor of this inference problem (Equation ??) is determined by the unknown variables  $f_{\rm life}$  and  $F_{\rm NUV,min}$ , as well as by the summary statistic Y (number of biosignature detections). To compute the distribution of evidences, we repeatedly generated samples under  $H_1$  and  $H_{\rm null}$  and computed the Bayes factors  $H_1$  and  $H_1$  and  $H_2$  we then evaluated the fraction of Monte Carlo runs in which certain evidence thresholds (?) were exceeded.

Under a more realistic scenario, the distribution of  $n_{\lambda}$  depends on additional planetary properties and their evolution, as well as on observational biases and sample selection effects of the survey. We will address these in the following section.

## 2.3. Exoplanet survey simulations with Bioverse

To assess the diagnostic power of realistic exoplanet surveys, we employed our survey simulator and hypotheses esis testing framework Bioverse (?). The general approach is as follows:

- 1. Exoplanet population synthesis: We populate the Gaia Catalogue of Nearby Stars (?) with synthetic exoplanets whose orbital parameters and planetary properties reflect our current understanding of exoplanet demographics (??). Here, we also inject the demographic trend in question in this case we assign biosignatures according to  $H_1$ , i.e., to planets in the HZ that have received NUV fluxes above a certain threshold.
- 2. Survey simulation: We simulate the detection and characterization of these exoplanets with a hypothetical survey, taking into account the survey's sensitivity, target selection, and observational biases. To model the sensitivity of the information gain of a proposed mission to sample selection and survey strategy, we conduct survey simulations with Bioverse using different sample sizes and survey strategies.
- 3. Hypothesis testing: We evaluate the likelihood that a given survey would detect a specified demographic trend in the exoplanet population and estimate the precision with which the survey could constrain the parameters of that trend. A common definition of the null hypothesis  $H_{\text{null}}$ , which is also applied here, is that there is no relationship between the independent variable (here: maximum NUV flux) and the dependent variable (here: biosignature occurrence). The alternative hypothesis  $H_1$  proposes a specific relationship between the independent and dependent variables. Bioverse offers either Bayesian model comparison or non-parametric tests to evaluate the evidence for or against the null hypothesis.

To determine the diagnostic capability of a given survey, Bioverse runs multiple iterations of the simulated
survey and calculates the fraction of realizations that
successfully reject the null hypothesis. We used this
metric, known as the statistical power, to quantify the
potential information content of the survey, identify critical design trades, and find strategies that maximize the
survey's scientific return.

#### 2.3.1. Simulated star and planet sample

We generated two sets of synthetic exoplanet populations, one for FGK-type stars and one for M-type stars. The stellar samples are drawn from the Gaia Catalogue <sup>255</sup> of Nearby Stars (?) with a maximum Gaia magnitude <sup>256</sup> of 16 and a maximum stellar mass of 1.5 M<sub>☉</sub>. We in- <sup>257</sup> cluded stars out to a maximum distance  $d_{\rm max}$  that de- <sup>258</sup> pends on the required planet sample size. Planets were <sup>259</sup> generated and assigned to the synthetic stars following <sup>260</sup> the occurrence rates and size/orbit distributions of ?. <sup>261</sup> Following ?, we considered only transiting EECs with <sup>262</sup> radii  $0.8 \, S^{0.25} < R < 1.4$  that are within the HZ (see <sup>263</sup> Section ??). The lower limit was suggested as a min- <sup>264</sup> imum planet size to retain an atmosphere (?). For all <sup>265</sup> survey simulations and hypothesis tests, we repeated the <sup>266</sup> above in a Monte Carlo fashion to generate randomized <sup>267</sup> ensembles of synthetic star and planet populations (?).

#### 2.3.2. Habitable zone occupancy and UV flux

268

To construct a test the UV Threshold Hypothesis, we required that life occurs only on planets with sufficient past UV irradiation exceeding the origins of life threshold  $F_{\rm NUV,min}$ . Further, we required this flux to have lasted for a minimum duration  $\Delta T_{\rm min}$  to allow for a sufficient "origins timescale" (?). All commonly investigated origins-of-life scenarios require water as a solvent; we thus considered only rocky planets that may sustain liquid water on their surface, i.e., that occupy their host star's momentary HZ during the above period, as well as at the epoch of observation. To determine HZ occupancy, we took into account the evolution of the host star's luminosity and HZ boundaries.

The HZ describes a region around a star where a planet with Earth's atmospheric composition and climate feedbacks can maintain liquid water on its surface (e.g., ?????). Here, we adopted orbital distance estimates that define the HZ as the region between the runaway greenhouse transition, where the stellar instellation cannot anymore be balanced through infrared cooling to space (?), and the maximum greenhouse limit, corresponding to the maximum distance at which surface temperatures allowing liquid water can be maintained through a  $CO_2$  greenhouse effect (?????).

We used the parametrization in ? to derive luminosity and planetary mass-dependent distance limits of the HZ

To determine HZ occupancy, we interpolated the stellar luminosity evolution grid of ? using a Clough Tocher
lar luminosity evolution grid of ? using a Clough Tocher
lar luminosity evolution grid of ? using a Clough Tocher
lar luminosity evolution of ? using a Clough Tocher
lar pute the evolution of the inner (runaway greenhouse)
land outer (maximum greenhouse) edges as a function of
lar planet mass and stellar spectral type (?). Being a lolar luminosity evolution of the inner (runaway greenhouse)
lar luminosity evolution grid of ? using a Clough Tocher
lar luminosity evolution grid of ? using a Clough Tocher
lar luminosity evolution grid of ? using a Clough Tocher
lar luminosity evolution grid of ? using a Clough Tocher
lar luminosity evolution grid of ? using a Clough Tocher
lar luminosity evolution grid of ? using a Clough Tocher
lar luminosity evolution grid of ? using a Clough Tocher
lar luminosity evolution grid of ? using a Clough Tocher
lar luminosity evolution grid of ? using a Clough Tocher
lar luminosity evolution grid of ? using a Clough Tocher
lar luminosity evolution grid of ? using a Clough Tocher
lar luminosity evolution grid of ? using a Clough Tocher
lar luminosity evolution grid of ? using a Clough Tocher
lar luminosity evolution grid of ? using a Clough Tocher
lar luminosity evolution grid of ? using a Clough Tocher
lar luminosity evolution grid of ? using a Clough Tocher
lar luminosity evolution grid of ? using a Clough Tocher
lar luminosity evolution grid of ? using a Clough Tocher
lar luminosity evolution grid of ? using a Clough Tocher
lar luminosity evolution grid of ? using a Clough Tocher
lar luminosity evolution grid of ? using a Clough Tocher
lar luminosity evolution grid of ? using a Clough Tocher
lar luminosity evolution grid of ? using a Clough Tocher
lar luminosity evolution grid of ? using a Clough Tocher
lar luminosity evolution grid of ? using a Clough Tocher
lar luminosity evolution grid of ? using a Clough Tocher
lar luminosity evolution grid of ? using a Clough Tocher
l

For the NUV flux, we used the age- and stellar mass- dependent NUV fluxes in the HZ obtained by ?, which considers GALEX UV data in the wavelength range of 177–283 nm. We linearly interpolate in their measured grid, where we convert spectral type to stellar mass using the midpoints of their mass ranges  $(0.75\,\mathrm{M}_{\odot}$  for K stars,  $0.475\,\mathrm{M}_{\odot}$  for early-type M stars, and  $0.215\,\mathrm{M}_{\odot}$  for late- type M stars). Outside the age and stellar mass range covered in ?, we extrapolate using nearest simplex (see right panel of Figure ??).

We then determined which planets were both in the HZ and had NUV fluxes above  $F_{\rm NUV,min}$ . To avoid considering short transitional phases, we require this situation to last for a minimum duration  $\Delta T_{\rm min} \geq 1\,{\rm Myr}$ . We assigned the emergence **and persistence** of life to a random fraction  $f_{\rm life}$  of all temperate planets fulfilling these requirements. For the probability of a planet having detectable biosignatures,  $P({\rm bio})$ , the UV Threshold Hypothesis then states

$$_{\text{325}} \quad H_{1}: P(\text{bio}) = \begin{cases} 0, & F_{\text{NUV}} < F_{\text{NUV},\text{min}} \\ f_{\text{life}}, & F_{\text{NUV}} \ge F_{\text{NUV},\text{min}} \\ & \text{and in HZ for } \Delta t \ge 1 \,\text{Myr} \end{cases}$$
(8)

and the corresponding null hypothesis  $H_{\text{null}}: P(\text{bio}) = f_{\text{life}}$ , i.e., no correlation with UV flux.

## 2.3.3. Transit survey simulations

With the synthetic star and planet samples generated,
we used Bioverse's survey module to simulate noisy measurements of key observables with a transit survey. We
assumed a hypothetical mission that can target a large
planet sample with high photometric precision and conduct a biosignature search on these planets (e.g., ??).
The simulated survey was designed to measure planetary instellation (for HZ occupancy) with a precision of
% and host star effective temperature with a precision
of 50.0 K. The maximum past NUV flux a planet received can be determined within a precision of 5%. To
marginalize over choices of biosignatures and their demarginalize over choices of biosignatures and their desum assumed that any inhabited planet would show a biosignature detectable by the survey.

### 2.3.4. Hypothesis testing

344

To evaluate the evidence for correctly rejecting the null hypothesis, we employed the Mann-Whitney U test (?). This is a non-parametric test of the null hypothesis that two independent samples were drawn from a population with the same distribution and is in particular sensitive to one sample being stochastically greater than the other. We used the Mann-Whitney U test

362

Figure 2. Interpolated stellar luminosity evolution (left) and evolution of the NUV flux in the HZ (right) as a function of host star mass. Scatter points show age and host star mass of the transiting planets in the synthetic planet sample; crosses denote the estimated NUV values in ?. We show three evolutionary tracks for a threshold flux of  $F_{\text{NUV,min}} = 300.0\,\text{erg}\,\text{s}^{-1}\,\text{cm}^{-2}$  that occupy the HZ (yellow sections) and exceed the threshold NUV flux (red sections) at different times. Where these sections overlap (white rectangles), the requirements for abiogenesis are met and we assign a biosignature detection with probability  $f_{\text{life}}$ . Planet 1 is an EEC orbiting a K dwarf that never receives sufficient NUV flux for abiogenesis. Planet 2 and Planet 3 enter the HZ at different times and receive sufficient NUV flux for different durations until their respective host star evolves below the threshold.

409

433

 $^{352}$  to compare the distributions of NUV fluxes of planets  $^{353}$  with and without biosignatures. The implementation  $^{354}$  in Bioverse relies on the <code>scipy.stats.mannwhitneyu</code>  $^{355}$  function (?) and returns a p-value, for which we set a  $^{356}$  significance level of  $\alpha=0.05$  to reject the null hypothesis  $^{357}$  sis. For every hypothesis test, we repeated randomized  $^{358}$  survey realizations to estimate the fraction of successive ful rejections of the null hypothesis, i.e., the statistical  $^{360}$  power of the survey.

#### 3. RESULTS

#### 3.1. Semi-analytical assessment

In Section ??, we computed the probability for true positive evidence for  $H_1$  and  $H_{\rm null}$ , respectively (Equasions ??, ??). Figure ?? shows how these evidences are distributed for sample sizes 10 and 100, and how likely we are to obtain strong evidence ( $BF_{H_i,H_j} > 10$ ). For n = 10, strong true evidence for  $H_1$  ( $H_{\rm null}$ ) can be expected in  $\sim 30\,\%$  ( $\sim 40\,\%$ ) of all random experiments. In the majority of cases, the outcome of the survey will be inconclusive. The situation improves with larger samples: for n = 100, 80 % of random samples permit conclusive inference (strong true evidence) under either  $H_1$  or  $H_{\rm null}$ .

The expected resulting evidence further depends on the a priori unknown rate of life's emergence and persistence  $f_{\rm life}$  and on the NUV flux threshold. Figure ?? illustrates this dependency: For very low values of either parameter, samples drawn under the null pays or alternative hypotheses are indistinguishable and the Bayesian evidence is always low. Both higher  $f_{\rm life}$  and higher NUV flux thresholds increase the probability of obtaining strong evidence. Larger sample sizes enable this at lower values of these parameters.

So far, we have assumed random, uniform distribusins of  $f_{\rm life}$ ,  $F_{\rm NUV,min}$ , and  $F_{\rm NUV}$ . A high biosignature detection rate  $f_{\rm life}$  increases the evidence (see Equation ??) but a survey strategy cannot influence it. The same is true for  $F_{\rm NUV,min}$ , where again higher values increase the evidence as the binomial distribution for  $H_{\rm 1}$  gets increasingly skewed and shifted away from the one for  $H_{\rm null}$ . However, one might select exoplanets for which a biosignature test is performed based on a priori available contextual information (?) in order to maxim

mize the science yield of investing additional resources. For instance, the distribution of  $F_{\rm NUV}$  in the planet sample can be influenced by the survey strategy, and a targeted sampling approach could favor extreme values. We model this by distributing  $F_{\rm NUV}$  according to different Beta functions and introduce a selectivity parameter  $s \in ]-1,1[$  such that  $F_{\rm NUV} \sim Beta(1/10^s,1/10^s).$  Figure ?? shows how the probability of obtaining true strong evidence for  $H_1$  scales with selectivity s. For large samples, a high selectivity  $(s \sim 1)$  can increase the probability of obtaining true strong evidence from  $\sim 70\,\%$  for ability of obtaining true strong evidence from  $\sim 70\,\%$  for  $m_{\rm subs} = 0$  (random uniform distribution) to  $> 90\,\%$ .

### 3.2. Survey simulations with Bioverse

With HZ occupancy as a requirement for abiogenesis, and barring selection biases beyond stellar brightness, the host star distribution of inhabited planets in a
simulated transit survey is skewed toward later spectral
types. For a fixed planet sample size, the fraction of inhabited planets is highest for planets orbiting M dwarfs
due to the higher NUV fluxes in the HZ of these stars
(see Figures ??, ??). Their NUV fluxes are generally
highest at early times ≤ 100 Myr. These host stars, in
particular late subtypes, also provide extended periods
of increased NUV emission that overlap with times when
some of these planets occupy the HZ (see Figure ??), our
requirement for abiogenesis (see Equation ??). Thus −
under the UV Threshold Hypothesis − most inhabited
transiting planets in the sample orbit M dwarfs.

Here, we are interested in the statistical power of a transit survey with a plausible sample selection and size. In the following, we fix the sample size to 250 and consider two different survey strategies targeting FGK and M dwarfs, respectively. We further investigate the sensitivity of the survey to the a priori unknown threshold NUV flux  $F_{\rm NUV,min}$  and the **probability of life emerging and persisting**  $f_{\rm life}$ .

#### 3.2.1. Selectivity of simulated transit surveys

In Section ??, we showed that the probability of obtaining true strong evidence for the hypothesis that life only originates on planets with a minimum past NUV flux is sensitive to the distribution of sampled past NUV fluxes, i.e., the selectivity of the survey (compare Figure ??). For both surveys targeting M dwarfs and those

Figure 3. Obtaining true strong evidence with different sample sizes. Left: Probability to reach given evidence levels for  $H_1$  and  $H_{\text{null}}$  under sample sizes n = 10 (solid) and n = 100 (dashed). Vertical lines denote thresholds for "strong" evidence,  $BF_{H_i,H_j} > 10$ , and "extreme" evidence,  $BF_{H_i,H_j} > 100$ . Right: Probability of obtaining true strong evidence for  $H_1$  as a function of sample size n.

Figure 4. Probability of obtaining true strong evidence for different abiogenesis rates, NUV flux thresholds, and sample sizes. For each of these parameters, higher values increase the probability of yielding strong evidence.

Figure 5. Scaling of the probability of obtaining true strong evidence with sample selectivity. Left: Sampling distribution for different selectivity parameters s. Right: Resulting P(true strong evidence), where  $f_{\text{life}}$  and  $F_{\text{NUV,min}}$  are randomly drawn from a uniform distribution. Sampling more extreme values of  $F_{\text{NUV}}$  is more likely to yield strong evidence.

targeting FGK dwarfs, the maximum NUV distribution is rather unimodal. Applying the approach from Level Sect. ?? of fitting a Beta function to the distribution, we find rather low selectivities (see Figure ??), which is likely detrimental for statistical hypothesis tests.

#### 3.2.2. Expected biosignature pattern

445

472

473

A representative recovery of the injected biosignature pattern is shown in Figure ??. There, we assumed an abiogenesis rate of  $f_{\rm life}=0.8$  and a minimum NUV flux of  $F_{\rm NUV,min}=300.0\,{\rm erg\,s^{-1}\,cm^{-2}}$ . All injected biosignatures are assumed to be detected without false positive ambiguity, and the maximum NUV flux is estimated from the host star's spectral type and age with an uncertainty corresponding to the intrinsic scatter in the NUV fluxes in ?. This leads to a distribution of biosignature detections with detections increasingly occurring above a threshold inferred NUV flux. In this example case, the higher evidence than in the KGK sample lead to a higher evidence than in the M dwarf sample, where the majority of planets are above the threshold NUV flux. Figure ?? shows the fraction of inhabited planets un-

Figure ?? shows the fraction of inhabited planets under the UV Threshold Hypothesis for different threshold
NUV fluxes and for the limiting case of a probability
for life's emergence and persistence of  $f_{\rm life} = 1$ .
This fraction decreases sharply with increasing threshdold flux, as fewer planets receive sufficient NUV flux for
abiogenesis. Another effect responsible for this drop is
that some planets receive the required NUV flux only
dold before entering the HZ – this is especially likely for
dold M dwarfs. For the FGK sample, the fraction of inhabdold planets drops at lower threshold fluxes than for the
M dwarf sample.

## 3.2.3. Statistical power and sensitivity to astrophysical parameters

We now investigate the sensitivity of the achieved statistical power of our default transit survey to the a pritransit ori unconstrained threshold NUV flux  $F_{\rm NUV,min}$  and the abiogenesis and persistence rate  $f_{\rm life}$ . Figure ?? shows the statistical power as a function of these parameters for a sample size of N=250. Values of  $F_{\rm NUV,min}$  that lie between the extrema of the inferred maximum NUV flux increase the achieved statistical power of the survey, as in this case the dataset under the alternative hypothesis  $H_1$  differs more from the null hypothesis. Furthermore, higher  $f_{\rm life}$  increase the evidence for  $H_1$ .

Parameter space regions with statistical power above 90% lie at  $f_{\rm life} > 0.5$  and mostly at threshold NUV fluxes of  $\sim 200$ –400 erg s<sup>-1</sup> cm<sup>-2</sup>. Notably, the sensitivity of the M dwarf sample extends into the low NUV flux end due to the broader distribution of maximum past NUV fluxes in this sample. Here, the FGK sample is barely sensitive.

#### 4. DISCUSSION

A key question in the quest to understand the origins of life is which natural processes best explain how living matter spontaneously appears from nonliving matter (e.g., ?). Using astronomical methods, this question will likely not be testable for individual planets but rather for ensembles of planets. The cyanosulfidic scenario for the origins of life (?), in particular its predicted existence of a minimum NUV flux required for prebiotic chemistry, offers an opportunity to test an origins of life hypothesis with a statistical transit survey sampling planets with varying NUV flux histories. In the following, we discuss the prospects of testing the UV Threshold Hypothesis in light of our results.

### 506 4.1. Sampling strategy for testing a NUV flux threshold

In Sect. ??, we show that testing the UV Threshold Hypothesis suffers from 'nuisance' parameters that hamper inference through astronomical observations. Here,
these parameters are the unspecified value of the NUV
threshold hypothesized to exist under  $H_1$ , and the unknown probability of detectable life emerging on a habtiable planet  $f_{\text{life}}$ . While the inference of a planet's entire UV flux evolution is difficult (e.g., ?), the estimated
maximum NUV flux that a planet was exposed to may

Figure 6. Simulated transit surveys targeting FGK and M stars.

Top: Host stars of all transiting EECs and inhabited planets in a simulated transit survey. In the FGK sample, all EECs and all inhabited planets orbit K dwarfs. In an M dwarf sample of the same size, the fraction of inhabited planets is larger. Center: Distribution of inferred maximum past NUV flux in transit surveys targeting EECs around FGK and M stars, respectively. The best-fit beta distributions correspond to selectivities of  $s_{\rm FGK} = -0.47$  and  $s_{\rm M} = -0.02$ . Red areas show inhabited

planets for an abiogenesis rate of  $f_{\text{life}} = 0.8$  and a generic threshold NUV flux  $F_{\text{NUV,min}} = 300.0 \,\text{erg s}^{-1} \,\text{cm}^{-2}$ . Bottom: Recovered biosignature detections and non-detections of simulated transit surveys. The dashed line denotes  $F_{\text{NUV,min}}$ .

569

Figure 7. Fraction of inhabited planets for different threshold NUV fluxes under the UV Threshold Hypothesis if the abiogenesis rate  $f_{\rm life}=1$ . For all samples, the fraction of inhabited planets drops sharply with increasing threshold NUV flux due to the combined effects of never receiving sufficient NUV flux for abiogenesis or receiving it before entering the HZ.

be used as a proxy, at least if one is interested in a minimum threshold flux and makes the assumption that planetary surfaces offer protection against too high UV fig flux. Indeed, the distribution of the number of planets with detected biosignature in a particular sample of planets with inferred maximum NUV values  $F_{\rm NUV}$  depends on both the values of  $F_{\rm NUV,min}$  and  $f_{\rm life}$  as shown in equation ??.

In our semi-analytical analysis (Section ??), we  $_{525}$  project a possible test performed by a future observer 526 equipped with a sample of exoplanets with derived past 527 maximum NUV exposure for which biosignature detec-528 tion has been attempted. This is necessarily reductive 529 as this observer will have more knowledge about exper-530 imental conditions and will therefore be able to use this 531 information to guide hypothesis testing. For instance,  $_{532}$  we have made the choice to consider the total number of 533 detected biosignatures as our summary statistic (Equa-534 tion ??), which is not sufficient to infer  $F_{NUV,min}$  and  $f_{life}$  separately. However, by conditioning the Bayes 536 factor to these variables (Equation ??), we calculate the 537 probability distribution of the Bayesian evidence in fa-538 vor of  $H_1$ . In doing so, we may evaluate how evidence 539 depends on the uncertainty over these unknown parame-540 ters in general terms, without assuming which particular 541 test a future observer might actually choose to perform 542 over real data when available. From this, we can see that target selection can strongly affect the conclusiveness of 544 a future test of the UV Threshold Hypothesis.

The particular finding that prioritizing extreme values of past NUV flux can enhance statistical power likely clashes with observational constraints, as the composition of the subset of planets that we can observe and for which detection of biosignature can be attempted is not independent from their NUV flux history. Hence, for our future observer, selectivity and sample size may be in conflict. This trade-off can be quantified in terms

553 of expected evidence yield, which we have done in Sec-554 tion ??. Our analysis shows that regardless of selec-555 tivity, sample sizes smaller than 50 likely result in in-556 conclusive tests, and that increasing selectivity towards  $_{557}$  extreme  $F_{
m NUV}$  offers limited inference gains compared 558 to the uniform case (s=0; Figure ??). For larger sam-<sub>559</sub> ples, however, a narrow distribution of  $F_{\rm NUV}$  may pre-560 vent inference entirely. We thus argue that selecting a  $_{561}$  sample with  $F_{
m NUV}$  distributed uniformly or emphasiz-562 ing extreme values should – barring any practical coun-563 terarguments – be considered in any future attempt at 564 testing the UV Threshold Hypothesis. Since the prac-565 tical implementation of an exoplanet survey can stand 566 in the way of such a selection, the following discussion 567 focuses on the results of our transit survey simulations with Bioverse. 568

Here, rather than simulating the full pipeline infer-571 ence, we focus on the Bayes ratio, which ignores consid-572 erations of prior distributions. The Bayes factor emerges 573 from the expression of the ratio between the posterior 574 evidence of  $H_1$  and the posterior evidence for  $H_0$ , al-575 lowing to cancel out the problematic term of the prior 576 probability of the observation. In addition, the par-577 ticular exercise of prospectively assessing the evidence 578 yield of different sampling or observation strategies Our 579 Bayes factor analysis quantifies how much evi-580 dence future data may provide in favor of a hy-581 pothesis against another one (the null hypoth-582 esis). Typical frequentist (p-value based) tests 583 usually evaluate only the likelihood of the null 584 hypothesis, thus requiring that the experiment be carefully crafted such that rejection of the null 586 hypothesis can be interpreted in favor of a par-587 ticular studied hypothesis (for instance that samples from coin tosses score a very low likelihood 589 under the hypothesis of a fair coin may indicate 590 that the coin is biased). In contrast, Bayes factor 591 analyses such as ours introduce additional con-592 straint to the testing by involving the likelihood of the tested alternate hypothesis (equation ??). 594 Thus, under Bayes-factor analyses, evidence for 595 the tested hypothesis is not only measured by 596 how unlikely the null hypothesis is given some 597 observation but rather by how much more likely

Figure 8. Statistical power as a function of threshold NUV flux and abiogenesis rate. Even for a large sample (here: N=250), a high statistical power of the transit survey requires high rates of life emerging and persisting  $f_{\rm life}$ . Intermediate values of  $F_{\rm NUV,min}$  are more likely to yield strong evidence than extreme values. For  $f_{\rm life} \gtrsim 80 \,\%$ , the sensitivity of the M dwarf sample extends into the low NUV flux end.

than the null hypothesis is the alternate hypothesis esis. The most exhaustive form of hypothesis selection test would be performed by using the entire Bayes theorem (equation ??), computing the posterior probability of the tested hypothesis. Doing so enables to quantify the information gain from performing some observation (by comparing the posterior with the prior), and to perform inference with consideration for prior information.

$$P(H_i|X) = \frac{P(X|H_i)P(H_i)}{P(X)}$$
(9)

609 However, implementing the Bayes theorem can 610 prove difficult in practice, owing to the (usually) 611 subjective nature of prior distributions. 612 prior distributions are required for the compu-613 tation of the posterior distribution: the prior 614 distribution for the considered model and hypothesis, and the prior distribution for the obser-616 vation. While the former requires that at least 617 some amount of consensus is identifiable in the 618 community of scientists that discuss this hypoth-619 esis, the latter also requires that either empirical 620 distributions for the prior distribution of the ob-621 servation be available or that the exhaustive list 622 of mechanistic pathways that could potentially 623 lead to this observation be known and tractable. 624 Taking the ratio of the posterior evidence for two 625 alternate hypotheses (i.e. of equation ??) allows 626 this problematic term, the prior probability for 627 the observation, to cancel out (equation ??).

$$\frac{P(H_1|X)}{P(H_0|X)} = \frac{P(X|H_0)P(H_0)}{P(X|H_0)P(H_0)}$$
(10)

628

This trades off the opportunity to estimate the posterior probability of a specific hypothesis with the possiblity to narrow down the problem to two specific competing hypotheses. Could there be factors other than the past UV flux that would determine the occurrence rate of biosignatures in terrestrial exoplanets? Surely, there is a vast array of possible mechanisms that could be considered which could shape the prior probability of an observed sample of biosignatures X. Truncating the ratio of prior probabilities from equation ?? results in the Bayes factor (equation ??), which we used in our semi-analytical

analysis (section ??). While the Bayes ratio only paints part of the picture of what a full inference pipeline would look line in a future survey aimed at testing origin of life hypotheses from the observation of biosignatures, it captures an essential part of the yield of a particular strategy: by how much would these observations tip the scale relative to prior expectations.

Here, rather than simulating the full pipeline inference, we focus on the Bayes ratio, which ignores considerations of prior distributions. The Bayes factor emerges from the expression of the ratio between the posterior evidence of  $H_1$  and the posterior evidence for  $H_0$ , allowing to cancel out the problematic term of the prior probability of the observation. In addition, the particular exercise of prospectively assessing the evidence yield of different sampling or observation strate-

## 4.2. How planetary context may constrain the UV Threshold Hypothesis

It comes to no surprise that the success rate for testing 664 the UV Threshold Hypothesis is sensitive to the sam-665 ple size of the survey and to the occurrence of life on 666 temperate exoplanets. As we have shown, the statisti-667 cal power of this test also depends on the distribution 668 of past NUV fluxes in the sample and on the threshold flux. Optimizing the survey to sample a wide range 670 of NUV flux values, particularly at the extremes, can 671 enhance the likelihood of obtaining strong evidence for 672 or against the hypothesis. Intermediate values of the 673 threshold NUV flux are more likely to yield strong ev-674 idence than extreme values, as the dataset under the  $_{675}$  alternative hypothesis  $H_1$  differs more from the null hy-676 pothesis in this case while still being sufficiently popu-677 lated. The threshold flux is, of course, a priori unknown 678 and we cannot influence it. If, however, better theoreti-679 cal predictions for the required NUV flux for abiogenesis become available (?), the survey strategy can be further optimized, for instance by targeting planets that are es-682 timated to have received a NUV flux slightly below and above this threshold or by applying a bisection algorithm 684 in a sequential survey (?).

### 4.3. An M dwarf opportunity

An interesting aspect lies in the distribution of host star properties, as different spectral types probe dif-

ferent past NUV flux regimes. FGK stars show a narrow distribution of maximum past NUV fluxes in the HZ, which may — depending on the (unknown) threshold NUV flux — limit the diagnostic power of a survey. In the case of a pure FGK sample, it will essentially only be sensitive to NUV flux thresholds  $\sim 200-400\,\mathrm{erg\,s^{-1}\,cm^{-2}}$ , and the chance of detecting biosignatures diminishes rapidly for higher thresholds within this range (see Figure ??). Detected biosignatures in an FGK sample would have little constraining power on testing the UV Threshold Hypothesis; they would either suggest that low NUV fluxes are sufficient for abiogenesis or indicate a different abiogenic pathway (e.g., ?). A lack of biosignatures in a larger FGK sample would support the UV Threshold Hypothesis.

On the other hand, M dwarfs show a wider distribution of maximum past NUV fluxes in their HZs. While
old M dwarfs can be considered low-UV environments,
a significant fraction of them emit high NUV fluxes into
their HZ during their early stages, in particular later
subtypes (?). This will help to test the high NUV flux
end of the UV Threshold Hypothesis; a higher occurrence of biosignatures here would support the hypothesis
that a higher NUV flux is favorable or necessary for life.
At the same time, a fraction of host stars in our M dwarf
sample extends it to lower maximum past NUV fluxes,
enabling tests of the low NUV flux end of the hypothesis.
The higher and more variable NUV fluxes in M dwarfs
thus increase the likelihood of obtaining strong evidence

The combination of a lack of UV radiation today, which makes biosignature gases more detectable (?), and a UV-rich past that may have enabled abiogenesis could make M dwarfs the preferred targets for biosignature searches. We note that relevant mission concepts, such as the Large Interferometer for Exoplanets (LIFE, ??), include M-dwarf systems among their primary targets (??). Our findings underscore the importance of constraining the UV emission profiles of EEC host stars throughout their evolutionary stages to assess the viability of M-dwarf planets as testbeds for theories on the origins of life (??).

## 4.4. Sensitivity to astrophysical parameters

Our Bioverse simulations that take into account exoplanet demographics, the evolution of habitability and NUV fluxes, and observational biases show that not only the likelihood of a conclusive test of the UV Threshold Hypothesis, but also the likelihood of successful biosignature detection itself is extremely sensitive to the threshold NUV flux if the hypothesis is true. Even if all biosignatures can be detected and the nominal rate of 739 life's emergence and persistence is very high, say  $f_{\rm life} = 1$ , under the condition that prebiotic chemistry 741 requires a minimum NUV flux and liquid water, if the 742 threshold flux turns out to be high the probability of 743 finding life on a randomly selected planet may be very 744 low. As we showed, for high required fluxes the two re-745 quirements of simultaneous HZ occupancy and sufficient 746 NUV flux conspire to diminish the fraction of inhabited 747 planets in the sample. Taking the inferred fluxes from? 748 at face value (but taking into account intrinsic scatter),  $_{749}$  a minimum required NUV flux of  $\gtrsim 400\,\mathrm{erg\,s^{-1}\,cm^{-2}}$  re-750 duces the fraction of inhabited planets to below  $\sim 1\%$ . 751 This not only calls for a large sample size and a tar-752 geted sample selection preferring high expected past 753 NUV fluxes, but also highlight the necessity of contin-754 ued theoretical and experimental research into the role 755 of UV radiation in prebiotic chemistry (???).

## 4.5. Contextual support for potential biosignature detections

757

782

The predicted interplay of NUV flux and HZ occurage pancy in enabling abiogenesis via the cyanosulfidic scenario could in principle be used to add or remove credibility from a tentative biosignature detection. For example, with a strong belief that this scenario is the only viable one for the origins of life, a biosignature detection on a planet orbiting a strongly UV-radiating star may add credibility to the detection. Conversely, a biosignature detection on a planet estimated to have received very little UV radiation would increase the likelihood of a false positive detection. On the other hand, should the detection in the latter case be confirmed, it could be used to falsify the UV Threshold Hypothesis.

Our simulations find no clear criterion for the credibility of a biosignature detection based on spectral type of
the host star, as both FGK and M dwarf samples show
similar maximum past NUV flux distributions. The
abiogenesis rate in both samples show similar trends
with the threshold NUV flux, and the fraction of inhabited planets drops at similar threshold fluxes (see
Section ??). A potentially inhabited planet's host star
spectral type may thus not be a strong indicator for the
credibility of a biosignature detection in the context of
the UV Threshold Hypothesis.

# 4.6. Overall prospects for testing the UV Threshold Hypothesis

Our results show that the UV Threshold Hypothesis is testable with potential future exoplanet surveys, but that the success of such a test depends on the sample size, the distribution of past NUV fluxes, and several unknown astrophysical nuisance parameters. Even under idealized conditions, obtaining strong evidence for or

790 against the hypothesis likely requires sample sizes on the 791 order of 100 (see Section ??). This is true for a future 792 transit survey, the specifics of which we have reflected in 793 our Bioverse simulations (see Section ??). However, we 794 have shown that the impacts from the combined require-795 ments of the UV Threshold Hypothesis on the fraction 796 of inhabited planets in a sample are comparable in the 797 non-transiting case.

Given the challenging nature of detecting and charac-799 terizing small (Earth-sized) exoplanets, most exoplanet mission concepts currently under development or consid-801 ered lack the potential for characterizing large enough 802 samples. Ground-based 25-40-meter class extremely large telescopes are expected to have the capabilities to 804 detect biosignatures on exoplanets like Proxima Cen-805 tauri b (e.g., ????). ? used Bioverse to determine 806 potential yields for a 10-year direct imaging and high-<sup>807</sup> resolution spectroscopy survey of O<sub>2</sub> on the Giant Mag-808 ellan Telescope (GMT) and on the Extremely Large Telescope (ELT) and found that between 7 and 19 habitable zone Earth-sized planets could be probed for Earth-811 like oxygen levels. Such a sample is too small to test 812 the UV Threshold Hypothesis, but it may be synergis-813 tic with other detection methods.

The Habitable Worlds Observatory (HWO) is ex- $_{815}$  pected to characterize a sample of  $\sim~25$  Earth analogs (??). Depending on the technical design, LIFE 817 is expected to target 25-80 EECs (??), which could be 118 just sufficient to constrain the UV Threshold Hypothe-819 sis. One current exception is the Nautilus Space Obser-820 vatory concept (??). Nautilus aims to characterize up <sub>821</sub> to  $\sim 1000$  EEC via transmission spectroscopy, building 822 on an innovative optical technology. To guide the defi-823 nition of future biosignature surveys, it is important to 824 refine predictions on the role of UV radiation in prebi-825 otic chemistry with both theoretical and experimental 826 work.

#### 4.7. Caveats

827

828

831

Our work is based on a number of assumptions and simplifications that may affect the results and conclu-829 830 sions. We discuss some of these caveats here.

? speculated that UV photochemistry might be rate-832 833 limiting for abiogenesis, particularly on planets orbit-834 ing M dwarfs, due to their lower baseline UV fluxes. This could delay abiogenesis by orders of magnitude, re-836 sulting in a continuous dependence of abiogenesis likeli-837 hood on UV flux. However, recent studies challenge this view for the cyanosulfidic scenario. ? calculated pho-839 tochemical timescales on early Earth at 180-300 hours 840 (7.5-12.5 days), significantly shorter than the timescale 841 for stochastic geological events (?). Even with 1000x 842 slower photochemistry on M-dwarf planets, abiogenesis 843 would occur within 20-30 years — geologically negligi-844 ble compared to stochastic processes — supporting the 845 step-function model.

Nonetheless, alternative abiogenesis pathways or com-847 binations of pathways may exhibit continuous or mixed 848 dependencies on UV flux. While the step-function for-849 malism is justified for the cyanosulfidic scenario, future 850 work should explore UV dependencies across other scenarios to refine predictions for biosignature distributions 852 and testable hypotheses.

## 4.7.1. The UV Threshold Hypothesis as a narrow step function

853

854

A key aspect of the UV Threshold Hypothe-856 sis is the proposed step-function dependence of 857 abiogenesis likelihood on UV flux. This approach 858 stems from the constraints governing photo-859 chemical pathways, which exhibit a threshold be-860 havior: below a certain flux, competing thermal reactions dominate, preventing abiogenesis, 862 while above the threshold, UV photochemistry proceeds at sufficient rates, and other stochastic 864 processes become rate-limiting.

speculated that UV photochemistry might be rate-limiting for abiogenesis, particularly on 867 planets orbiting M dwarfs, due to their lower baseline UV fluxes. This could delay abiogenesis by orders of magnitude, resulting in a continu-870 ous dependence of abiogenesis likelihood on UV 871 flux. However, recent studies challenge this view 872 for the cyanosulfidic scenario. ? calculated pho-873 tochemical timescales on early Earth at 180-300 874 hours (7.5-12.5 days), significantly shorter than the timescale for stochastic geological events (?). 876 Even with 1000x slower photochemistry on M-877 dwarf planets, abiogenesis would occur within 878 20-30 years — geologically negligible compared 879 to stochastic processes — supporting the stepsso function model.

Nonetheless, alternative abiogenesis pathways 882 or combinations of pathways may exhibit contin-883 uous or mixed dependencies on UV flux. While 884 the step-function formalism is justified for the 885 cyanosulfidic scenario, future work should explore UV dependencies across other scenarios to 887 refine predictions for biosignature distributions sss and testable hypotheses.

#### 4.7.2. Existence of an atmosphere-crust interface

By its nature, cyanosulfidic scenario relies on rock 891 surfaces exposed to the planetary atmosphere. Water

914

worlds that have their entire planetary surface covered by oceans contradict this requirement and do not allow for the wet-dry cycling inherent to this origin of life scenario. The competition of tectonic stress with gravitational crustal spreading (?) sets the maximum possible height of mountains, which in the solar system does not exceed ~20 km. Such mountains will be permanently underwater on water worlds. Another impediment to wet-dry cycles may be tidal locking of the planet as it stalls stellar tide-induced water movement and diurnal irradiation variability (e.g., ?). However, recent dynamical models suggest tidally locked planets to undergo rapid drift of their sub-stellar point (?).

### 4.7.3. Stellar flares

Our assumptions on past UV flux neglect the contribution of stellar flares, which may be hypothesized as an alternative source of UV light (??). This concerns mainly ultracool dwarfs, due to their low quiescent emission and high pre-main sequence stellar activity (??). However, recent work indicates that the majority of stars show inadequate activity levels for a sufficient contribution through flares (???).

#### 4.7.4. Atmosphere transmission

We do not take into account absorption of UV radia-915 916 tion by the planetary atmosphere. Theoretical work sug-917 gests that the atmosphere of prebiotic Earth was largely 918 transparent at NUV wavelengths with the only known 919 source of attenuation being Rayleigh scattering (??). 920 We thus approximated surface UV flux using top-of-921 atmosphere fluxes. If there are planets in a sample 922 that do not have a transparent atmosphere at NUV 923 wavelengths and require higher fluxes for abiogenesis, 924 the fraction of inhabited planets in the sample will be 925 lower. However, these planets will not pollute the below-926 threshold subsample, as they will not be able to host life 927 under the UV Threshold Hypothesis. Exoplanet surveys 928 focusing on highly irradiated planets offer an opportu-929 nity to constrain the typical oxidation state of rocky exoplanets, providing insights into the average composi-931 tion of their secondary atmospheres (?). This is partic-932 ularly relevant for prebiotic worlds, as varying oxidation 933 states significantly perturb the classical habitable zone 934 concept (?) and also influence surface UV levels through 935 changing atmospheric transmission. Optimally, the at-936 mospheric composition of young rocky protoplanets will be probed to constrain the possible range of atmospheric 938 and mantle oxidation states during early planetary evo-939 lution by future direct imaging concepts (?).

We propose that specific origins-of-life scenarios may leave a detectable imprint on the distribution of biosignatures in exoplanet populations. We have investigated the potential of upcoming exoplanet surveys to test the hypothesis — motivated by the cyanosulfidic origins-of-life scenario — that a minimum past NUV flux is required for abiogenesis. To this end, we first employed a semi-analytical Bayesian analysis to estimate probabilities of obtaining strong evidence for or against this hypothesis. We then used the Bioverse framework to assess the diagnostic power of realistic transit surveys, taking into account exoplanet demographics, time-dependency of habitability and NUV fluxes, observational biases, and target selection.

Our main findings are:

955

957

958

959

960

961

962

964

965

966

967

968

969

970

971

972

973

974

975

977

978

979

980

981

982

983

- The UV Threshold Hypothesis of the cyanosulfidic scenario for the origins of life should lead to a correlation between past NUV flux and current occurrence of biosignatures that may be observationally testable.
- 2. The required sample size for detecting this correlation depends on the abiogenesis rate on temperate exoplanets and the distribution of host star properties in the sample; in particular their maximum past NUV fluxes. Samples smaller than 50 planets are unlikely to yield conclusive results.
- Under the UV Threshold Hypothesis, the fraction of inhabited planets in a transit survey is sensitive to the threshold NUV flux and is expected to drop sharply for required fluxes above a few hundred erg s<sup>-1</sup> cm<sup>-2</sup>.
- 4. If the predicted UV correlation exists, obtaining strong evidence for the hypothesis is likely ( $\gtrsim 80\%$ ) for sample sizes  $\geq 100$  if the abiogenesis rate is high ( $\gtrsim 50\%$ ) and if no very high NUV fluxes are required. A survey strategy that targets extreme values of inferred past NUV irradiation increases the diagnostic power.
- 5. Samples of planets orbiting M dwarfs overall yield higher chances of successfully testing the UV Threshold Hypothesis. They may also be more likely to yield biosignature detections under this hypothesis.

Overall, our work demonstrates that future exoplanet surveys have the potential to test the hypothesis that a minimum past NUV flux is required for abiogenesis. More generally, we found that models of the origins of life provide hypotheses that may be testable with these surveys. Conducting realistic survey simulations with representative samples is important to identify testable science questions, support trade studies, help define science cases for future missions, and guide further theoretical and experimental work on the origins of life. Our work highlights the importance of understanding the context in which a biosignature detection is made, which can not only help to assess the credibility of the detection but also to test competing hypotheses on the origins of life on Earth and beyond.

#### ACKNOWLEDGMENTS

The authors thank Kevin Heng, Dominik Hintz, 1000 and Rhys Seeburger for insightful discussions. This 1002 material is based upon work supported by the Na-1003 tional Aeronautics and Space Administration under Agreement No. 80NSSC21K0593 for the program "Alien Earths". The results reported herein bene-1006 fited from collaborations and/or information exchange within NASA's Nexus for Exoplanet System Science (NExSS) research coordination network sponsored by 1009 NASA's Science Mission Directorate. This work has 1010 made use of data from the European Space Agency 1011 (ESA) mission Gaia (https://www.cosmos.esa.int/gaia), 1012 processed by the Gaia Data Processing and Analysis 1013 Consortium (DPAC, https://www.cosmos.esa.int/web/ 1014 gaia/dpac/consortium). Funding for the DPAC has 1015 been provided by national institutions, in particular 1016 the institutions participating in the Gaia Multilateral 1017 Agreement. T.L. was supported by the Branco Weiss 1018 Foundation, the Netherlands eScience Center (PRO-1019 TEUS project, NLESC.OEC.2023.017), and the Alfred 1020 P. Sloan Foundation (AEThER project, G202114194).

#### AUTHOR CONTRIBUTIONS

1021

M.S., D.A., and S.R. conceived the project, planned 1022 its implementation, and interpreted the results. M.S. developed the planetary evolution component to Bioverse, 1025 carried out the hypothesis tests and statistical analyses, and wrote the manuscript. D.A. leads the "Alien Earths" program through which this project is funded, 1028 helped to guide the strategy of the project, and provided text contributions. A.A. carried out the semi-analytical 1030 computations regarding the correlation of past UV flux and biosignature occurrence. S.R. advised on planetary 1032 NUV flux evolution and the cyanosulfidic scenario of the 1033 origins of life. R.F. wrote the initial draft of the Intro-1034 duction and advised on the evolutionary biology aspects 1035 of the project. K.H.-U. contributed to the Bioverse soft-1036 ware development and simulations. T.L. supported the 1037 selection of testable hypotheses and provided text con-1038 tributions to the initial draft. S.M. advised on the scope

of the project and supported the selection of testable hypotheses. All authors provided comments and suggestions on the manuscript.

1042

#### REPRODUCIBILITY

All code required to reproduce our results, figures, and this article itself is available at https://github.com/matiscke/originsoflife.